EUROPEAN ORGANIZATION FOR NUCLEAR RESEARCH
ORGANISATION EUROPEENNE POUR LA RECHERCHE NUCLEAIRE

CERN - LHC & PS DIVISION

LHC/VAC Note 2001-007
PS/AE Note 2001-009

RESULTS FROM FIRST EXPERIMENT TO MEASURE LEAD ION INDUCED DESORPTION AT LINAC3

J. Hansen, J. M. Laurent, N. Madsen and E. Mahner

Geneva, Switzerland
July 4, 2001

Contents

1 Introduction

In November and the beginning of December 2000, a series of experiments were carried out at LINAC3 in order to measure the molecular desorption caused by impact of 4.2 MeV/u lead ions. This note is a short summary of the results of the experiment as well as some preliminary conclusions with respect to the design of the Low Energy Ion Ring (LEIR) vacuum system, and what further experiments it would be profitable/necessary to carry out.

2 Experimental Setup

An overview of the experimental setup used for the measurements is shown in Figure 1. LINAC3 delivers shots of $\sim 10^{10}$ Pb^{27+} ions with a length of 560 μs. The shots can be delivered either continuously with a repetition rate of 1.2 s or on request (single shot) using a PS-Booster cycle for triggering (usually SFTION). For LEIR purposes the main interest is Pb^{53+}, and to obtain Pb^{53+} the Pb^{27+} ions are sent through a stripping foil. The stripping process results in pulses of $\sim 1.5 \cdot 10^9$ Pb^{53+} ions.

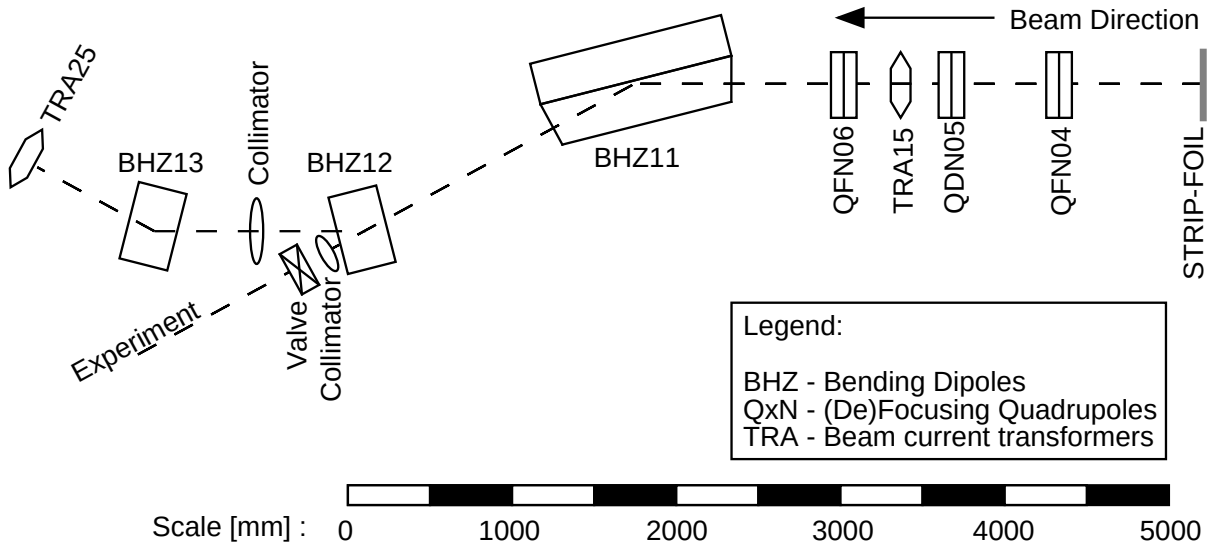

Figure 1: Overview of the experimental setup at LINAC3. The beam goes from right to left, the drawing starting with the stripping foil on the right.

Figure 1 also shows that after the stripping foil a few magnetic elements are positioned. The three quadrupoles are used for controlling the beam size and divergence in the test chamber [3]. After the quadrupoles a dipole magnet bends the beam towards the experiment and serves to spatially separate the different charge states emanating form the stripping process. A collimator is used to select the desired charge state to be injected into the test chamber.

Figure 2 shows a more detailed drawing of the experimental setup which has been connected to LINAC3 after the collimator, the beam moves from right to left. A sector valve separates the linac from the experimental setup such that the test chamber may be changed without disturbing the linac. After the sector valve a pump chamber has been connected to a long narrow chamber. The narrow chamber serves two purposes. First of all, it separates the high pressure of the linac from the test setup. Secondly, as the test chamber is pumped through this long narrow chamber,

the chamber serves to give a known pumping speed which is independent of the state of the Ti-Sublimation and the Ion pump which are attached at the pump chamber.

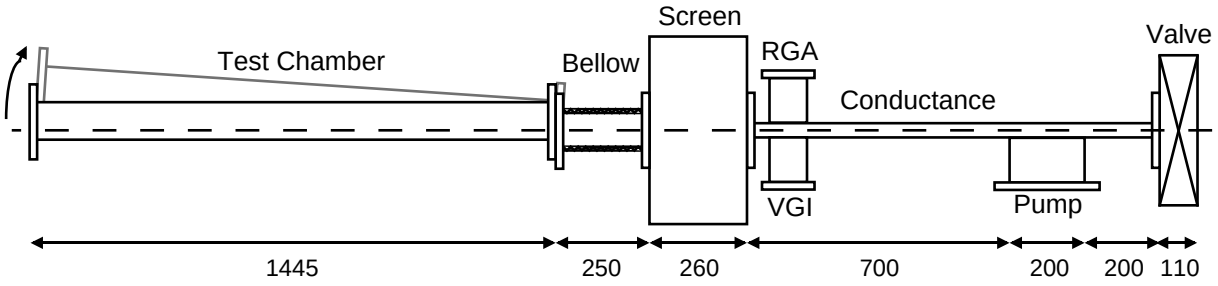

Figure 2: The experiment which has been attached to LINAC3 for the ion induced desorption measurements. Distances are given in mm.

Right before the test chamber two measurement chambers are connected. The first serves for an ionization gauge to measure the total pressure in the test chamber and a residual gas analyzer (RGA). The second and largest chamber contains a fluorescent screen which is used for aligning the beam into the test chamber. Not shown on Figure 2 are a pumping group and a gas dozing valve connected to the screen chamber. The test chamber itself is a long (due to the grazing incidence of the lead ions) stainless steel tube of inner diameter 145 mm. Three chambers with different pre-treatments have been tried in the experiment.

Chamber **A** : Standard chamber representing the standard treatment in the LEAR machine. The chamber was exposed to the CERN standard cleaning procedure (CERN/PS.TR01) and vacuum fired at 950°C. After installation the chamber was baked at 300°C for 24 hours.

Chamber **B** : After initial cleaning and vacuum firing like chamber A, the chamber was baked for 24 hours at 300°C, and thereafter exposed to Ar-O_2 Glow Discharge cleaning[1] with 0.8 A for 1.5 hours at 300°C. After this the chamber was baked at 350°C for 24 hours to remove the Ar from the surface [4]. The chamber was then vented with Nitrogen before being installed in the test stand. After installation the chamber was baked to 350°C for 24 hours.

Chamber **C** : After initial cleaning and vacuum firing like chamber A the chamber was coated with a Non-Evaporable Getter (NEG) of Ti-Zr-V. After installation the chamber was baked to 100°C for 36 hours during which the rest of the system was baked at 300°C. Next, the temperature was increased by 20°C/h to 200°C and left at 200°C for 24 hours in order to activate the NEG coating.

3 Experimental Results

The chambers have all been exposed to lead ion impact of Pb^{53+} and Pb^{27+}, for Pb^{53+} both with continuous injection every 1.2 s as well as single shot measurements. For the single shot measurements the pressure development was monitored using the residual gas analyzer with an integration time setting of τ= 250 μs. As will be shown in the results, this speed was necessary

[1]The gas mixture for the glow discharge was 90% Ar and 10% O_2.

to avoid the electronics of the RGA to integrate too much, and thereby distort the resulting pressure measurement. Three impact angles were investigated: Grazing incidence with 14 mrad and 90 mrad with respect to the surface and perpendicular incidence on the end flange of the test chamber.

3.1 Settings of the Residual Gas Analyzer

The electronics of the RGA integrates the ion current signal in order to reduce noise. Partial pressure measurements were carried out where the time scale of relevance could be as small as 10 ms. Therefore, a number of partial pressure measurements where carried out for different settings of the RGA speed.

Figure 3 shows the results of a series of measurements of the ion current development versus time after a Pb^{53+} shot for various settings of the RGA integration time.

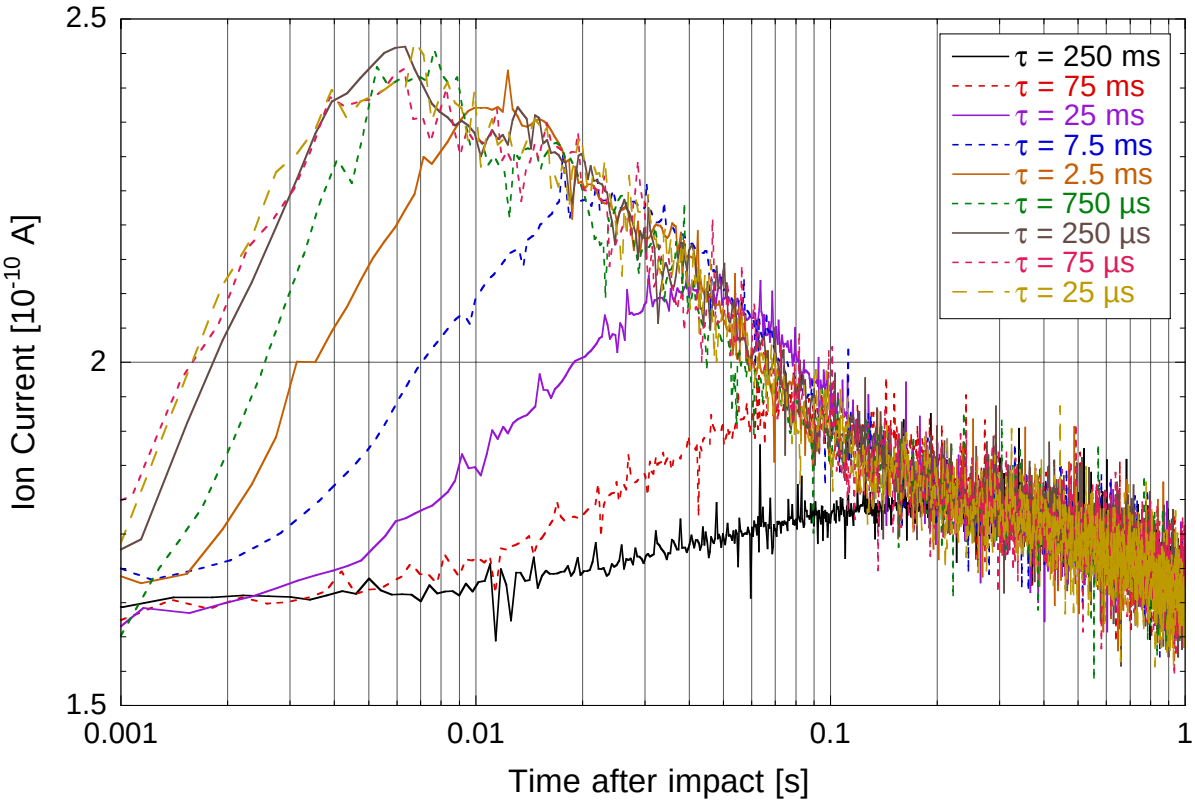

Figure 3: Measurement of the development of the m/q =28 peak with the RGA as a function of time after the impact of a shot of Pb^{53+} when chamber A was exposed to repeated pulses every 1.2 s. The inset gives the RGA setting (integration time of the electronics) for the various measurements.

The measurements in Figure 3 lead to the use of a setting of 250 μs/u as the standard setting for this kind of measurements, as one observes that the change between 25 μs and 250 μs is negligible. The integration time of the electronics is thus shorter than the time scale of the pressure development.

To extract the molecular desorption yield from measurements as the above the ideal gas law may be used. The ideal gas law is a law for a gas in equilibrium. Equilibrium in this context means that the changes in the gas occur on a time scale much longer than the mean molecular

transit time in the vacuum system. The heaviest molecule studied is CO_2, which at 300 K has a thermal velocity of $\sim$240 m/s. The length of our system is about 2 m, which gives maximum transit times of the order of 10 ms. Care should therefore be taken in drawing conclusions from changes occurring faster than about 100 ms (an order of magnitude from the transit time). It is however interesting to observe that the 10 ms calculated above is about the rise time of the partial pressure of CO. The shot length of 560 μs is furthermore short compared to the other time scales and can thus be ignored in this regard.

3.2 Equilibrium Measurements

In LEAR ions were lost quasi continuously, thus the first investigation to carry out on the various chambers and with various impact angles is to measure the change in the equilibrium pressure in the test chamber when exposed to continuous bombardment of lead ions.

Figure 4 shows an example of a measurement of the total (N_2 equivalent) pressure in the chamber under various experimental conditions including continuous bombardment with lead ions.

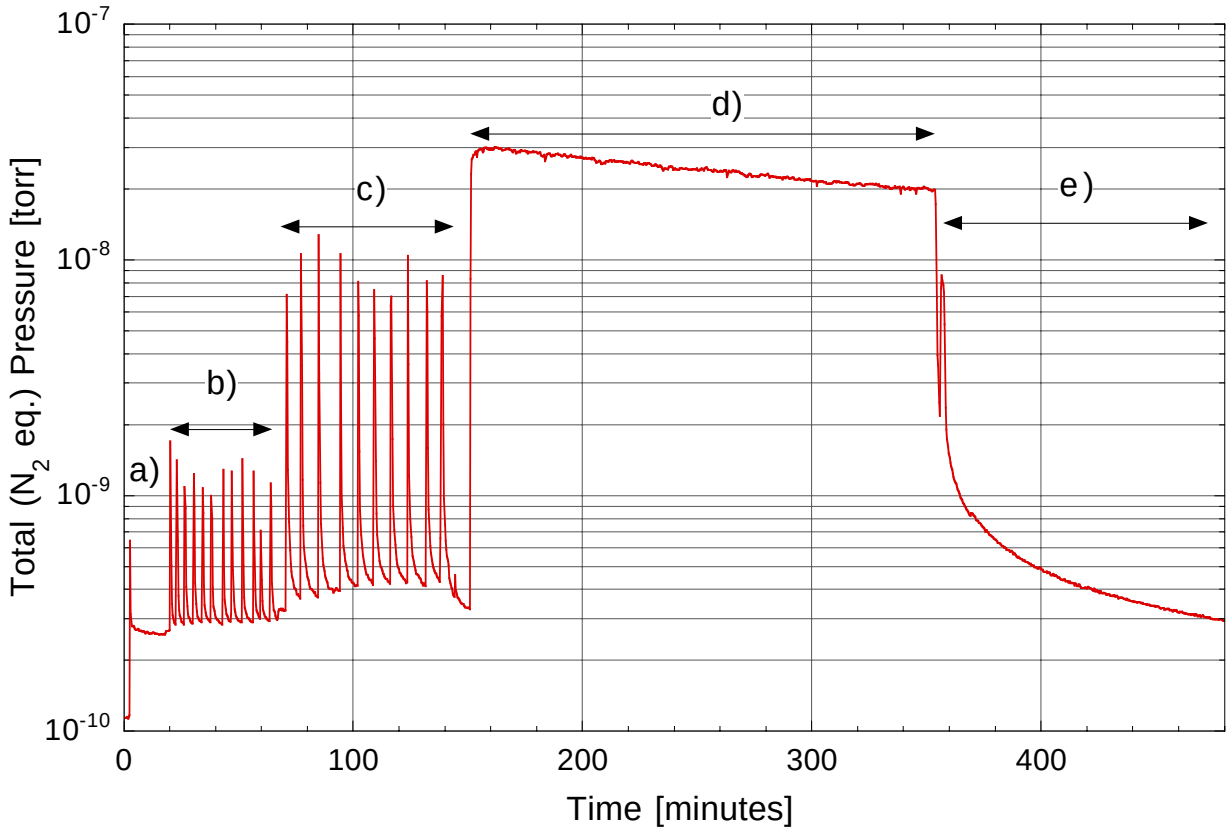

Figure 4: Pressure in test chamber A during a period in the experiment. The particles impacted with 14 mrad grazing incidence. a) A sector valve separating the experimental line from the LINAC3 is opened. The pressure in LINAC3 is higher than the base pressure in the experiment. b) A series of single shots of $1.5{\cdot}10^9$ Pb^{53+} ions. The time between the shots is the time needed for the vacuum to return to the conditions before each shot. c) A series of single shots of $1.0{\cdot}10^{10}$ Pb^{27+} ions. d) Pb^{53+} shots are injected with a repetition rate of 1.2 s. e) The ion beam was switched off, and the pressure decayed. The short pressure increase right after the beam was switched off arose because the sector valve was closed.

From the measurement shown in Figure 4 one finds that the loss of about $1.3{\cdot}10^9$ Pb^{53+} ions/s cause a pressure increase of a factor 91. With the calculated pumping speed of 26.8 L/s (for H_2) this results in a desorption yield η of $2.0{\cdot}10^4$ molecules per incident Pb^{53+} ion. The reported pressure increase in LEAR was a factor 5 for a loss rate of about $5{\cdot}10^7$ ions lost per second, from which a desorption yield of $5{\cdot}10^5$ molecules per incident Pb^{54+} was estimated [3]. A factor 20 difference is thus observed between the experiment reported here and the LEAR situation, however the uncertainty on the LEAR estimate is rather large as the pumping speed was unknown, thus the result reported here seems thus anyhow to confirm that the pressure increase observed in LEAR is due to lost lead ions. It has been calculated that the lost ions impact mainly with grazing incidence (14 mrad at the extreme) [3]. However, theory indicates that less grazing incidence (or even perpendicular) incidence give smaller desorption yields. Measurements of the yield with 90 mrad grazing incidence and perpendicular incidence were therefore also carried out.

The cleaning effect evident in Figure 4 during the repeated shots has not been observed during the LEAR experiments. However, the intensity per unit area on the surface in LEAR was more than a factor 100 smaller, thus careful investigations would have been necessary to observe this.

The equilibrium pressure under continuous Pb^{53+} bombardment has been measured for three angles and for all three chambers. Table 1 summarizes the results.

Chamber	Unexposed	Perpendicular	90 mrad	14 mrad
A	$2.5{\cdot}10^{-10}$ torr	$3.7{\cdot}10^{-9}$ torr ($\times$15)	$1.3{\cdot}10^{-8}$ torr ($\times$42)	$2.9{\cdot}10^{-8}$ torr ($\times$91)
B	$3.9{\cdot}10^{-10}$ torr	$1.3{\cdot}10^{-8}$ torr ($\times$33)	$4.3{\cdot}10^{-8}$ torr ($\times$109)	$1.5{\cdot}10^{-7}$ torr ($\times$333)
C	$8.0{\cdot}10^{-11}$ torr	$4.0{\cdot}10^{-10}$ torr ($\times$5)	$4.0{\cdot}10^{-10}$ torr ($\times$5)	$1.3{\cdot}10^{-9}$ torr ($\times$16)

Table 1: Absolute and relative pressure rise in the test chambers when exposed constantly to shots of $1.5{\cdot}10^9$ Pb^{53+} ions every 1.2 seconds for three different incidence angles.

The results shown in Table 1 support the earlier assumption that grazing incidence of 14 mrad desorbs the most molecules from the surface. It is also observed, that the pressure in the NEG coated chamber is lower than in the other chambers. However, the pressure of the NEG coated chamber is not more than a factor five lower than chamber A. This is surprising, as the NEG coating should increase the pumping speed by a factor 50-100 and therefore equivalently reduce the pressure. This observation therefore suggests that the outgassing of chamber C is larger than for the other chambers. A further surprise is that the Ar-O_2 glow discharged chamber B is not better than the standard chamber A - rather significantly larger pressures are observed in chamber B.

3.3 Single Shot Measurements

For each angle and chamber as well as for both charge states +27 and +53 measurements of the partial pressure of the major gases as a function of time after impact of a single shot of ions were carried out. As discussed earlier, we should be careful in drawing conclusions of partial pressure changes that occur at time scales faster than 100 ms. The RGA integration time was set to τ=250 μs for all these measurements.

Figure 5 shows an example of a collection of partial pressure measurements. The RGA can be set to monitor only one m/q peak at a time, thus the partial pressures shown in the figure are calculated assuming that the shots are reproducible. The reproducibility was tested several times during the experiment. The partial pressures in all cases have have been calculated using the formula

$$\begin{bmatrix} P_{H_2} \\ P_{CH_4} \\ P_{CO} \\ P_{Ar} \\ P_{CO_2} \end{bmatrix} = \begin{bmatrix} 16.234 & 0 & 0 & 0 & 0 \\ 0 & 46.887 & 0 & 0 & 0 \\ 0 & 0 & 42.373 & 0 & -24.788 \\ 0 & 0 & 0 & 62.5 & 0 \\ 0 & 0 & 0 & 0 & 77.519 \end{bmatrix} \times \begin{bmatrix} I_{m/q=2} \\ I_{m/q=15} \\ I_{m/q=28} \\ I_{m/q=40} \\ I_{m/q=44} \end{bmatrix} \quad (1)$$

where P_X is the partial pressure of species X, and $I_{m/q=a}$ is the ion current measured with the RGA set to $m/q = a$. The entries in the conversion matrix were extracted from an *in situ* calibration of the RGA [6].

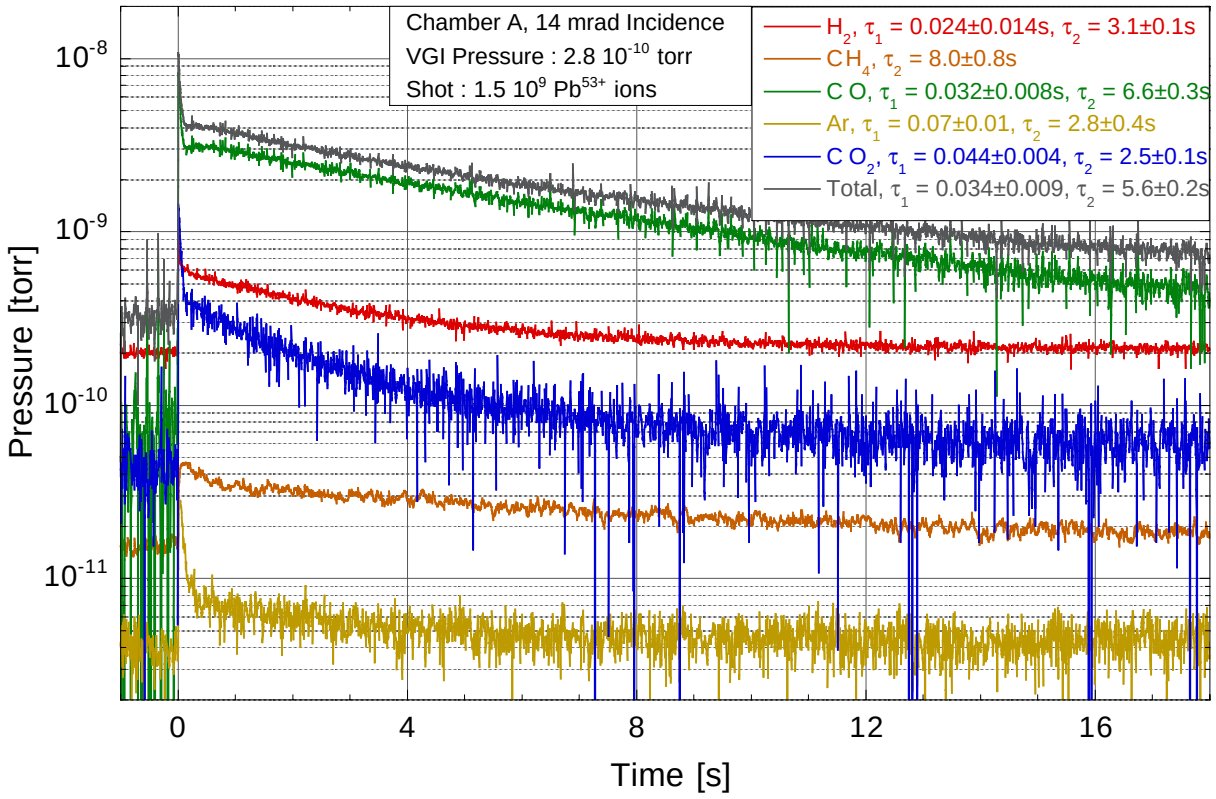

Figure 5: Partial pressures measured for chamber A with $1.5{\cdot}10^9$ incident Pb^{53+} ions at 14 mrad grazing incidence. The decay times shown in the legend result from two exponential fits to the pressure decays. τ_1 is the result from the fit to the fast part of the decay.

Several interesting features may be extracted from Figure 5. The decays of the various partial pressures have been fitted with exponential decays, from these rates an estimate of the pumping speed of the different gases can be extracted. However, as the fits depend rather a lot on the exact part of the function which is fitted the extracted pumping speeds may only be used as a rough guideline. With a total test chamber volume (this includes the 'screen' chamber and the measurement chamber and the bellow) of 76 L, the pumping speeds from the various measurements on chamber A may be found. Table 2 gives the pumping speeds measured for the various

cases. Only the slow part (τ_2) of the pumping in Figure 5 has been included in the table. The fast decay observed right after injection has a time scale close to the molecular transit times in our system which makes it difficult to quantize. The fast decay was however observed reproducibly, and for both chamber A and B, thus it is believed to represent some physical effect but we do not presently have enough information to speculate as to the nature of the process behind this observation. The calculated pumping speed in Table 2 has been found assuming that it is limited by the conductance of the 700 mm×ø35 mm tube connecting the pump chamber with the test chamber [3].

Ion	Angle	Individual Pumping Speeds [L/s]				
		S_{H_2}	S_{CH_4}	S_{CO}	S_{Ar}	S_{CO_2}
Pb^{53+}	Perp.	23.8	13.1	14.1	11.9	58.5
Pb^{53+}	90 mrad	23.8	10.1	14.9	N.A.	76.0
Pb^{53+}	14 mrad	24.5	9.5	11.5	27.14	30.4
Pb^{27+}	Perp.	30.4	11.2	15.5	27.1	N.A.
Pb^{27+}	90 mrad	29.9	9.6	14.3	63.3	70.4
Pb^{27+}	14 mrad	26.2	9.2	10.0	24.5	26.2
Calculated		26.8	9.5	7.2	6.0	5.7

Table 2: Estimated pumping speeds extracted from fits to measurements on chamber A. The pumping speeds of chamber B are very similar. Note that the noise on the Ar partial pressure measurement is large compared to the pressure change due to pumping. The pumping speed estimate for Ar is therefore very uncertain.

The correspondence between the theoretical and the measured pumping speeds given in Table 2 is quite good, apart from the pumping speeds of Ar and CO_2. As we normally have very little Argon in the chamber this gives an extra twist of uncertainty, and it may be that this pumping is dominated by sticking (re-adsorption on the surface). CO_2 is usually present in abundance, thus only sticking seems to be responsible for the discrepancy. However, for the low masses the measured decay rates are in good agreement with the calculated values.

The agreement between the pumping speed extracted from the single shot measurements and the theoretically expected pumping is good. We therefore conclude that the single shot measurements are a good means to measure the desorption yields. The pumping speeds are however not quite good enough to be used to calculate the desorption yield, however another method is possible.

3.3.1 Desorption Yields

The next issue to address from these measurements is thus the desorption yield. Even though, as may be seen on Figure 5, pressure changes on time scales of tens of milliseconds were observed the desorption yield has been calculated from the difference between the peak pressure of the gas in question and the mean pressure right before impact of the lead ions. The yield has been calculated using the ideal gas law[2]

$$\eta = \frac{\Delta P \cdot V}{N_{Pb} k_B T} \tag{2}$$

[2]This implies the assumption that there is zero pumping.

where V=76 L is the test volume, k_B the Boltzmann constant, T=300 K the temperature and N_{Pb} the number of impacting lead ions. Implicitly this means, that it has been assumed, that the number of molecules desorbed is proportional to the number of lead ions. This has not been tested directly, but during the experiment the current varied sometimes by up to 20%, and no indication of stronger than linear dependency on current was observed.

Ion	Angle	Desorption Yields [Molec./Pb ion]					
		η_{H_2}	η_{CH_4}	η_{CO}	η_{Ar}	η_{CO_2}	Total
Pb^{53+}	Perp.	861	44	7128	14	1805	9852
Pb^{53+}	90 mrad	662	31	5382	9	1234	7318
Pb^{53+}	14 mrad	1570	51	13294	39	2276	17230
Pb^{27+}	Perp.	92	4	816	2	222	1136
Pb^{27+}	90 mrad	135	9	868	2	220	1233
Pb^{27+}	14 mrad	557	41	4357	7	613	5575

Table 3: Desorption yields of the main desorbed gases under lead ion impact on chamber A.

Table 3 shows that the main component desorbed is CO. This was also observed in LEAR, and this observation is the reason for the test of the Ar-O_2 glow discharge as this cleaning method earlier has been observed to remove Carbon very efficiently from the surface. It is also evident that grazing incidence of 14 mrad has the highest desorption yield, as was also expected from sputtering experience, which however has been done at much lower energies (keV/u, this was briefly discussed in Ref. [2]). The total desorption yield measured with this method is in agreement with the yield extracted from the equilibrium measurements under exposure of the chamber to ion shots every 1.2 s. On a more physical note we observe that the desorption yield of Pb^{27+} is significantly lower that for Pb^{53+}, the difference being the smallest at 14 mrad gazing incidence, where it is a factor 3. We have no available theory to describe the process in detail, but for sputtering processes one often observes a quadratic scaling in the charge. The observed change of the desorption yield with a doubling of the charge lie between a factor 8.6 and 1.3, showing significant variation with the angle of incidence.

Measurements similar to those summarized in Table 3 have been carried out for chamber B and C. A comparison of the development of the CO partial pressure for the three chambers is shown in Figure 6.

Ion	Angle	Desorption Yields [Molec./Pb ion]					
		η_{H_2}	η_{CH_4}	η_{CO}	η_{Ar}	η_{CO_2}	Total
Pb^{53+}	Perp.	888	41	7580	305	1662	10477
Pb^{53+}	90 mrad	1188	42	8108	2161	2053	13552
Pb^{53+}	14 mrad	1493	46	9699	8950	2288	22476
Pb^{27+}	Perp.	122	5	927	92	259	1404
Pb^{27+}	90 mrad	118	1	2061	851	497	3528
Pb^{27+}	14 mrad	239	19	8452	6449	1927	17086

Table 4: Desorption yields of the main desorbed gases under lead ion impact on chamber B.

From the desorption yield measurements, summarized in Table 4 and 5, a couple of conclusions may be drawn. First of all one observes that the desorption yields of the Ar-O_2 glow

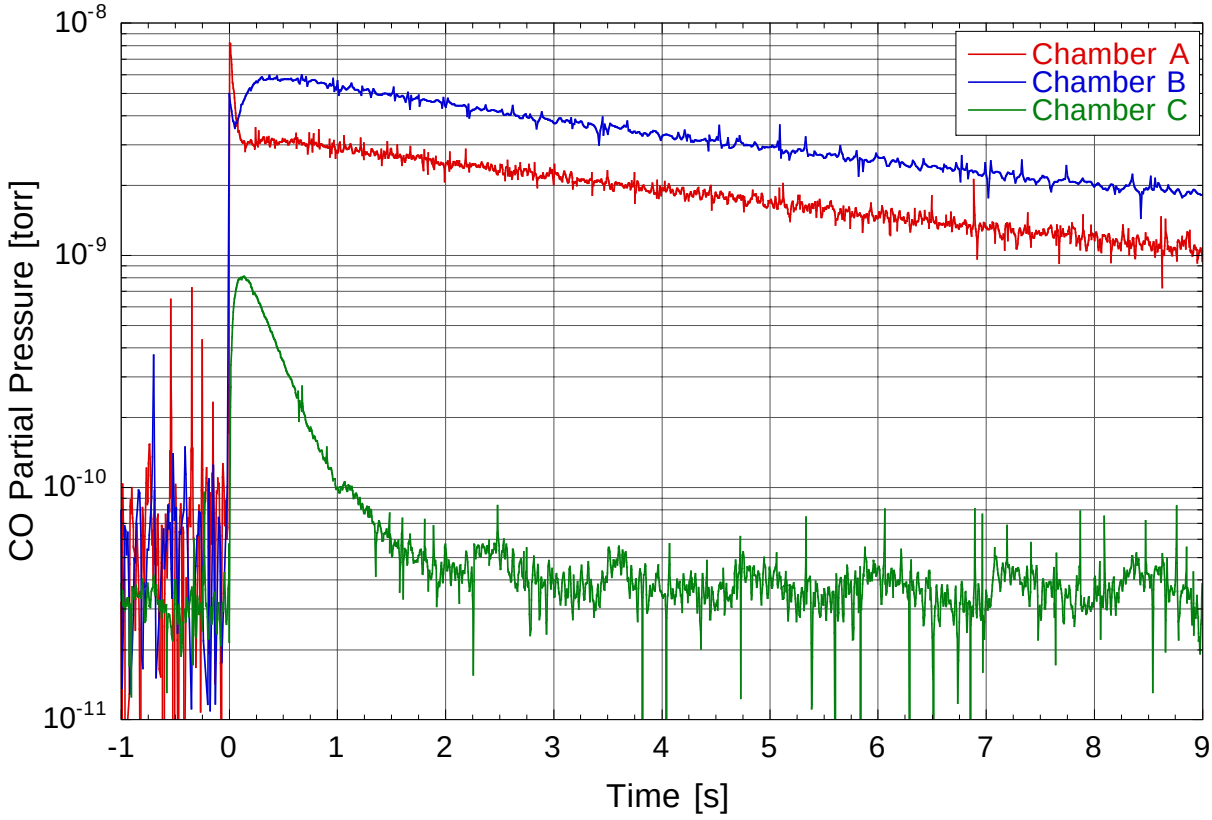

Figure 6: CO partial pressure development for the three different chambers measured with pulses of $1.5{\cdot}10^9$ Pb^{53+} ions at 14 mrad grazing incidence.

discharged tube have not been reduced as expected, rather they are more or less similar to those of chamber A, apart from the desorption yield of Argon which has increased by two orders of magnitude. Figure 7 shows a comparison between the desorption yields of the different chambers and gases for 14 mrad grazing incidence.

Secondly, we observe that the yields of chamber C (NEG coated) are slightly smaller than for chamber A, but not with more than a factor two in the best case. However, the pumping speeds might be of interest. Table 6 shows a measurement, using a standard equilibrium with gas injection method, of the individual pumping speeds for chamber C. For chamber C the pumping speed can not be measured using the decay rate of the partial pressure of the different gases. The reason for this is that the sticking probability on a NEG surface is so high that the pressure measurement carried out in the RGA is not representative for the pressure development in the chamber. Therefore, only the pumping speed as measured using a standard equilibrium method are given in Table 6.

As the pumping speeds in this case are rather large compared to the time scale of molecular transit, the desorption yield measurements assuming zero pumping underestimate the actual desorption. Furthermore the large pumping speed confirms the functioning of the NEG, and therefore supports the earlier hypothesis that the residual outgassing of chamber C is higher than the others as the base pressure without bombardment was only a factor five lower than for the other chambers.

Ion	Angle	Desorption Yields [Molec./Pb ion]					
		η_{H_2}	η_{CH_4}	η_{CO}	η_{Ar}	η_{CO_2}	Total
Pb^{53+}	Perp.	775	35	4336	11	394	5551
Pb^{53+}	90 mrad	845	40	5109	9	368	6371
Pb^{53+}	14 mrad	1859	76	8750	39	1656	12380
Pb^{27+}	Perp.	169	6	1239	2	92	1507
Pb^{27+}	90 mrad	142	7	1109	2	252	1514
Pb^{27+}	14 mrad	330	50	1360	4	245	1988

Table 5: Desorption yields of the main desorbed gases under lead ion impact on chamber C.

S_{H_2} [L/s]	S_{CO} [L/s]	S_{Ar} [L/s]
$1.5 \cdot 10^3$	500	10

Table 6: Equilibrium measurements of the individual pumping speeds in chamber C. The measurements were carried out *in situ* using a standard pumping speed measurement method [7].

4 Conclusions

The following list of issues summarizes the results of the experiments carried out so far.

- The measurements show that with a loss of about $1.3 \cdot 10^9$ Pb^{53+} ions/s under 14 mrad grazing incidence the equilibrium pressure increases by two orders of magnitude. With the calculated pumping speed of 26.8 L/s this results in a desorption yield η of $2 \cdot 10^4$ molecules/Pb^{53+} ion. The estimated desorption yield from the LEAR pressure increase was $5 \cdot 10^5$ molecules per incident Pb^{54+} [3]. A factor 20 difference is thus observed between the experiment reported here and the LEAR situation, however the uncertainty on the LEAR estimate is rather large as the pumping speed was unknown, thus the result reported here seems thus anyhow to confirm that the pressure increase observed in LEAR is due to lost lead ions.

- Grazing incidence of 14 mrad yields more desorbed molecules than less grazing incidence or even perpendicular incidence. The difference between the two extremes has been observed to be a factor 2 for Pb^{53+} ions. Thus a change of the LEAR vacuum system causing the bulk of the lost lead ions to be lost under perpendicular impact may improve the dynamic vacuum by a factor 2.

- A significant dependence on the charge state of the lost ion has been observed. This indicates that the desorption process occurs rather close to the surface as an ion moving through a material quickly assumes an equilibrium charge state were electron loss and capture evens out, thereby loosing information about the initial charge state before impact. This knowledge has no real implications for the LEAR situation, but may well be important elsewhere.

- The Ar-O_2 glow discharge cleaning carried out on chamber B does not show any signs of having reduced the desorption yield. Furthermore, the chamber exhibits large Ar desorp-

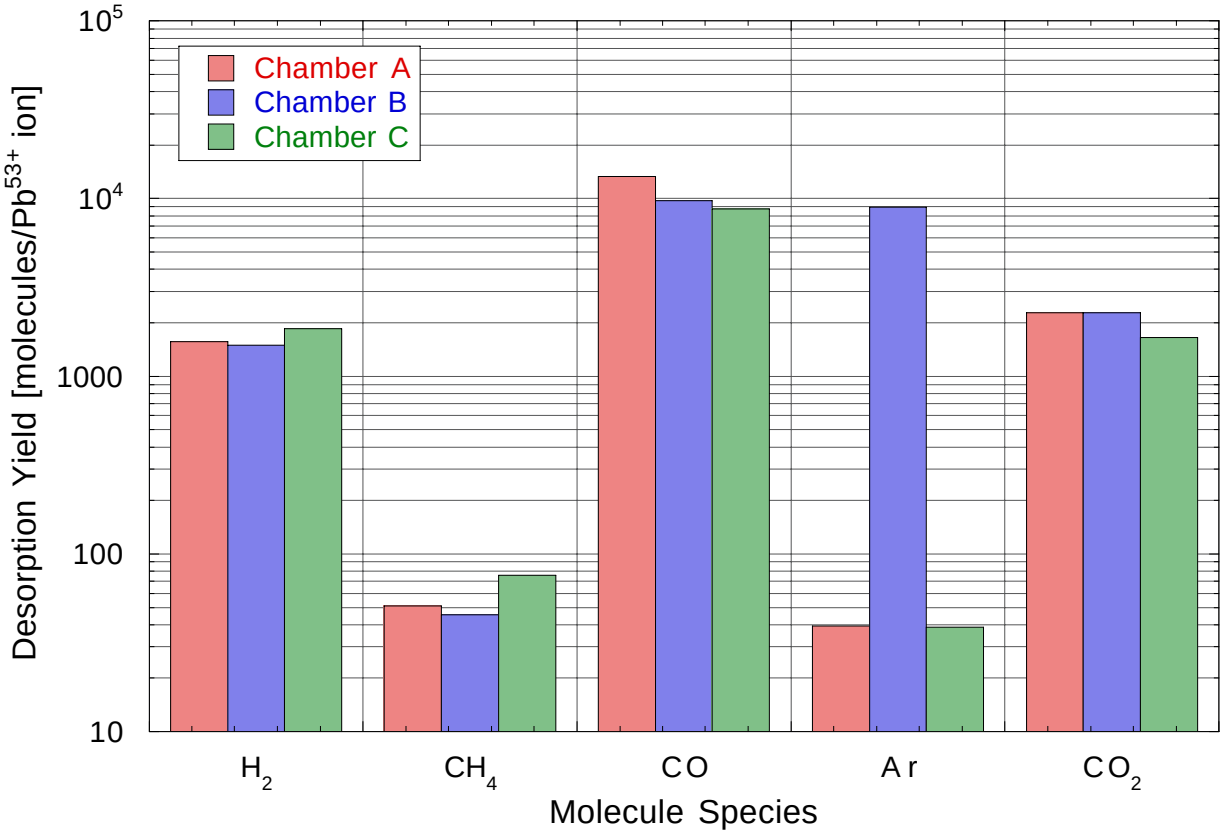

Figure 7: Desorption yields measured with single shots of $1.5{\cdot}10^9$ Pb^{53+} ions at 14 mrad grazing incidence. The yields were calculated using the ideal gas law and the instantaneous pressure increase due to the single shots. Pumping has thus been ignored in the calculation, and the desorption yield for chamber C are therefore underestimated.

tion yields indicating that the glow discharge mainly has resulted in Argon being implanted into the surface.

- The equilibrium pressure obtained with the NEG coating was only a factor 5 lower than for the other chambers, and as the pumping speed of the NEG was observed to be 50-100 times higher the out-gassing of the NEG surface must be about 10 times higher than for the A and B chamber surfaces. The desorption rate for the NEG coated chamber did not significantly differ from that of the other two chambers.

- Finally, we observe, in all cases that the bulk of the molecules desorbed are CO. CO_2 and H_2 are the second most abundant species in the desorbed gas. CO, which influence the beam lifetime 50 times more than H_2 contributes in fact 70 to 80% of the desorbed molecules. This means that not only does the loss of lead ions cause an increase in pressure, but also a worsening of the vacuum composition.

The cause for the LEAR pressure increase has been identified with certainty. With the present information the most likely scheme seems to be to use the fact that the losses are known to occur in the bending sections. With this knowledge it should be feasible to change the vacuum chambers such that most of the ions are lost with perpendicular impacts, reducing the out-gassing by a factor 2.

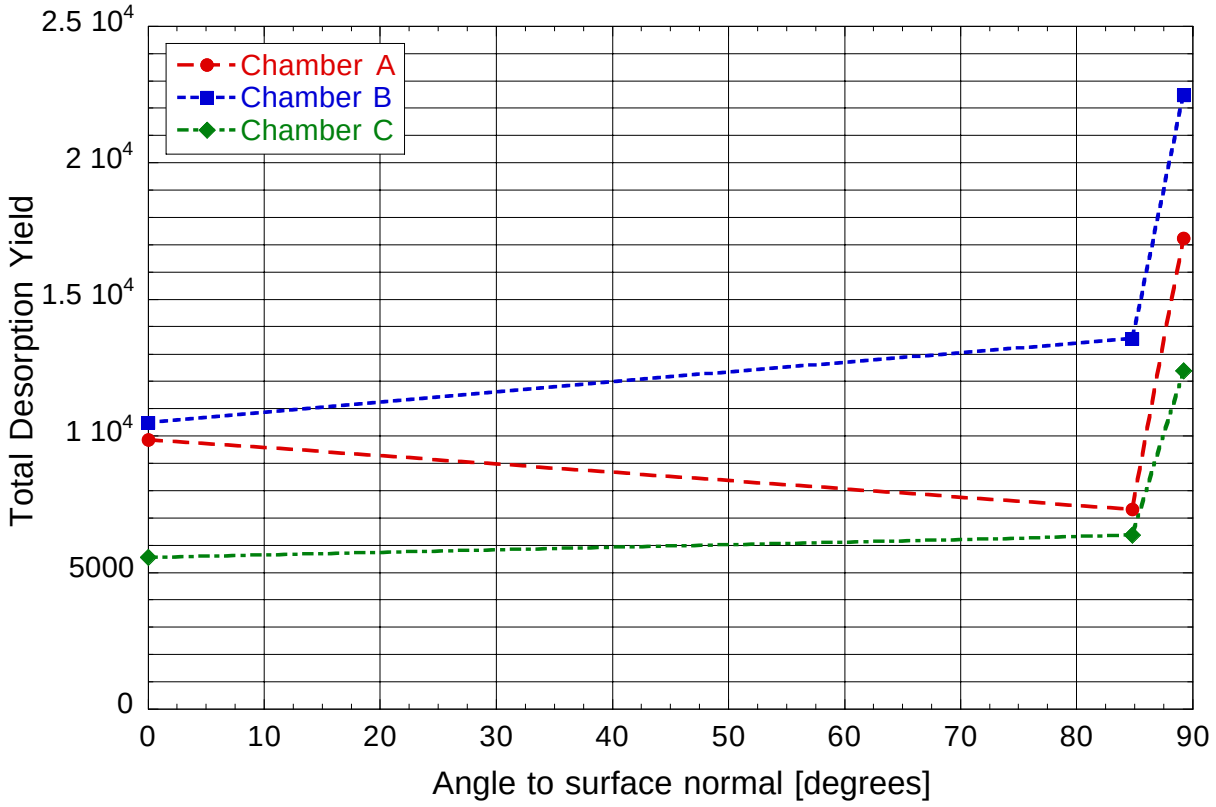

Figure 8: Total desorption yield η for the three different chambers as a function of the impact angle relative to the surface normal for impact of Pb^{53+} ions.

5 Outlook

The following points remain to be investigated.

- The lack of observation of a cleaning effect of the glow discharge treatment may indicate that the desorption takes place deeper in the surface. As some cleaning during the bombardment with lead ions was already observed, it would be interesting to investigate this further to see the magnitude of the effect.
- One necessary experiment is to check the proportionality of the out-gassing with the number of incident ions. The results so far obtained are measured with about 1000 times the intensity that existed in LEAR, thus a check of the linearity seems desirable. During the experiment the beam current varied up to 20%, and no indication of anything but linear scaling appeared, however it would make sense to be certain of this.
- The results obtained for the Ar-O_2 glow discharged chamber were disappointing. As this surface treatment has been very beneficial in the ISR it would be worthwhile to repeat the experiment and investigate whether Ar-O_2 glow discharge can in fact reduce the desorption yield. Other possibilities would be to try with other discharge gases [2, 4].
- The dynamic behavior of the measured partial pressure as a function of the RGA settings has been measured for CO only. In order to check the validity of the information extracted from these measurements it would be worthwhile to investigate the time scale of the pressure rise time as a function of the molecular species too.

- One interesting experiment would be to use a NEG coating baked at a higher temperature, as it is possible that the increased out-gassing in the experiment is due to the lower baking temperature.
- Another interesting possibility would be to carry out the experiment with a 'sawtooth' surface, which should secure that the ions impact with large angles to the surface.
- Finally it might be worthwhile to electropolish and chemically polish the surfaces of the chambers before the vacuum firing.

It should be kept in mind that the fundamental problem being faced here might be that the lost lead ions desorb molecules who are embedded deeper into the surface than any of the various surface cleaning methods can penetrate. If this is really the case, the solution to the vacuum problem may well be to install apertures in the LEIR vacuum cleaned before hand by 53+ MeV lead ions.

6 Acknowledgements

The experiments described in this note could not have been done without the help and assistance of many different people at CERN. The authors therefore would like to acknowledge the help of various people. Firstly, we would like to thank M. Chanel, O. Gröbner and D. Möhl for many fruitful discussions, suggestions and assistance both before and during the experiment. Secondly, we would like to thank the LINAC 3 team, C. Hill, D. Kuchler, M. O'Neil and R. Scrivens for making the linac available and useful to us. Furthermore, we would like to thank P. Chiggiato and P.C. Pinto for the NEG coating of chamber C. Finally, we are grateful for the technical support we have received both during setup and running of the experiment from D. Allard, C. Lacroix, K. Magyari, S. Southern and J. P. Pasquet and his team.

References

[1] J. Bosser, C. Carli, M. Chanel, C. Hill, A. Lombardi, R. Maccaferri, S. Maury, D. Möhl, G. Molinari, S. Rossi, E. Tanke, G. Tranquille and M. Vretenar, *Experimental Investigation of Electron Cooling and Stacking of Lead Ions in a Low Energy Accumulation Ring*, Internal note, CERN/PS 99-033 (DI), (1999)

[2] N. Madsen, *Vacuum changes during accumulation of* Pb^{54+} *in LEIR*, CERN internal note, PS/DI Note 99-21, November 1999

[3] N. Madsen, *Calculations for an Experiment to Measure Gas Desorption Induced by Impact of Lead Ions.*, CERN/PS/AE 2000-011, September 2000

[4] A.G. Mathewson, CERN-ISR-VA/76-5; A.G. Mathewson, CERN-ISR-VA/77-59; N. Hilleret, CERN/LEP-VA-NH (1984); A.G. Mathewson, CERN-LEP-VA/87-63

[5] S.Y. Zhang and L.A. Ahrens, *Gold Beam Losses at the AGS Booster Injection*, Proc. 1999 Particle Accelerator Conference, (New York, USA), 3294 (1999)

[6] J.-M. Laurent and K. Magyari, Private Communications, September 2000

[7] J.-M. Laurent and K. Magyari, *Mesure in-situ de vitesse de pompage au Linac 3*, CERN/LHC-VAC/JML/mpt(00-42), December 8, 2000